

## Polarization splay as the origin of modulation in the *B1* and *B7* smectic phases of bent-core molecules

D. A. Coleman, C. D. Jones, M. Nakata, and N. A. Clark

<sup>1</sup>*Liquid Crystal Materials Research Center and Department of Physics, University of Colorado, Boulder, Colorado 80309, USA*

D. M. Walba

*Liquid Crystal Materials Research Center, and Department of Chemistry, University of Colorado, Boulder, Colorado 80309, USA*

W. Weissflog

*Institut für Physikalische Chemie, Martin-Luther Universität Halle-Wittenberg, Muhlplforte 1, Germany*

K. Fodor-Csorba

*Research Institute for Solid State Physics and Optics, Hungarian Academy of Sciences, P.O. Box 49, H-1525 Budapest, Hungary*

J. Watanabe

*Department of Organic and Polymeric Materials, Tokyo Institute of Technology, O-okayama, Meguro-ku, Tokyo 152-8552, Japan*

V. Novotna and V. Hamplova

*Institute of Physics, Academy of Sciences of the Czech Republic, Na Slovance 2, 182 21 Prague 8, Czech Republic*

(Received 21 May 2007; published 8 February 2008)

We report a generalized scenario for the formation of modulated smectic phases of bent-core molecules based on locally ferroelectric layering and spontaneous splay of the polarization. Twelve phases are proposed, distinguished by neighboring splay stripes with either syn- or antiorder of the polarization and undulation slope, in addition to layer continuity versus layer discontinuity at the intervening defects. We outline the experimental techniques necessary to differentiate among the phases and interpret previous results in the present context, using high resolution x-ray scattering diffraction and block and undulation models of the layer organization to distinguish among the three 2D lattice types which emerge.

DOI: [10.1103/PhysRevE.77.021703](https://doi.org/10.1103/PhysRevE.77.021703)

PACS number(s): 61.30.-v, 61.05.cp

Bent-core smectic liquid crystals are known to exhibit spontaneously polar and chiral layers leading to the “*B2*” bilayer fluid smectic phases (*SmCPs*) which have four possible local layer structures depending upon the relative polarity and chirality of adjacent layers [1,2]. In addition to the *B2* phases, bent-core molecular systems exhibit closely related phases: the two dimensionally modulated *B7*, in this case a structure of continuous periodically undulated smectic layers [4]; and the *B1*, a structure of blocks of smectic layering organized into two-dimensional (2D) columnarlike lattices [5]. These undulated and columnar-like phases are often found to exhibit a beautiful characteristic set of textures in depolarized transmitted light microscopy, which suggests some commonality of organizational themes. The *B7* layer undulation was successfully interpreted as being the result of the deformation of a background *SmC<sub>S</sub>P<sub>F</sub>* *B2* phase by the tendency for local polarization splay, which leads in turn to the formation of a periodic array of polarization splay stripes spaced by intervening defects. In the *B7* phase the layers are continuous through the defects, but it was suggested in the same paper [4] and subsequently [3], that the *B1* could also be understood on the basis of polarization splay stripes, but with layer displacement steps at the defects [4].

Here we pursue this notion, reporting a polarization splay approach to understanding both the *B1* and *B7* phases, showing that, in fact, a variety of phases can be generated, some already observed and some yet to be found, depending on the

choice of the relative tilt and polarity of adjacent splay stripes and the nature of the interstripe defects. X-ray diffraction from these phases often exhibits one or two dominant Bragg reflections having very little temperature (*T*) dependence of peak position, accompanied by a collection of weak reflections that shift in position with changing *T*. We have developed a “block” model of such phases to account for this behavior, showing that it is a consequence of *T*-independent smectic layer spacing in blocklike stacks of layers, accompanied by *T*-dependant changes in block width and the orientation of layers relative to the stacking direction. Here we limit our considerations to either continuous layers or layer half-steps at the defects and use both layer undulation and layer block models to interpret the x-ray data. The resulting x-ray diffraction patterns compare favorably to data obtained on three distinct classes of *B7* and *B1* materials.

Figure 1(a) shows a columnar smectic block of the type proposed to constitute the basic unit cell of the *B1* phase, and illustrates the motivation for polarization splay as a driving force for generating 2D modulated bent-core smectic phases. In the *B1* phases the layers are displaced by a half-spacing at the defect boundaries. In the *B7* the layers are continuous but with the defects that reorient the polarization direction. In either case, at the *y-z* boundary surface of the block at the defect acquires a polar character parallel to *x*; thus the region at the boundary between stripes presents an environment that is structurally distinct from the region in the middle of the

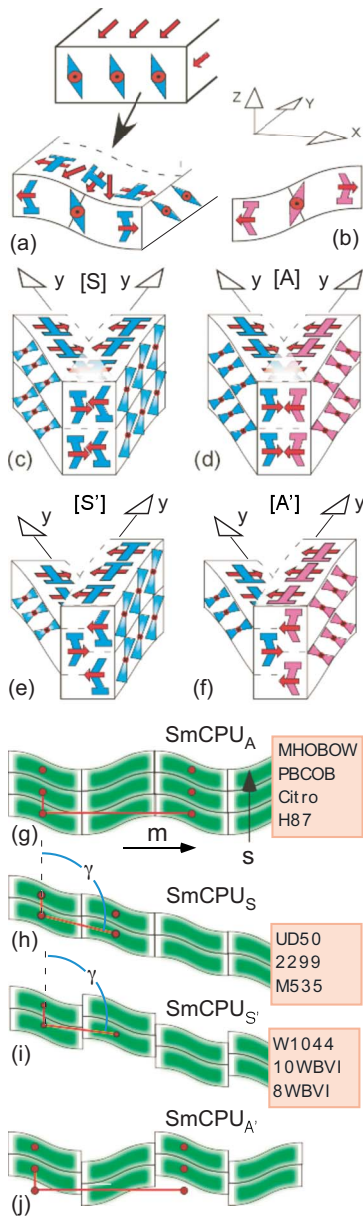


FIG. 1. (Color online) Polarization splay stripe. The polarization aligns along  $y$  in the middle of the stripe and splays outward at the edge of the stripe. The stripe undulates along  $x$  in order to accommodate the defects at  $x = \pm l/2$ . (b) Elastic energy is minimized if the layer undulates up if the molecules tilt to the right. Chirality can either be (c) preserved or (d) reversed across the defect. (e),(f) Interdigitated defects that induce a half-layer discontinuity in the layering. (g) A rectangular lattice in which stripes alternate between positive and negative slope. (h),(i) An oblique lattice results when all stripes have the same slope. (j) A rectangular lattice with interdigitated layer defects has not yet been observed.

stripe and so in general one end of the polar molecule will have a lower free energy within this region (a tendency for polar ordering along  $x$ ). This lowering of the free energy acts as an effective polar anchoring energy that tends to turn the polarization at the edge of the stripe either toward or away from the stripe edge, thereby imposing splay, in a fashion similar to that found in surface stabilized ferroelectric liquid crystal cells [4]. Thus, in any striped layer populated by polar

molecules with some component of the polar director oriented parallel to the stripe (along  $y$ ) must exhibit splay, i.e., the uniform block structure of Fig. 1(a) will deform to the splayed structure, as indicated by the arrow. The undulation will appear as an additional consequence of the difference in layer spacing between the defect and stripe center regions. Since in the  $B7$  case we were able to account for the appearance of phase on the basis of a local tendency for splay of  $P$ , we make a similar proposal here, namely the  $B1$  phases are also driven by polarization splay, with the different structures found produced by the possibilities afforded by different defect structures and motifs of chirality and polarity.

Polarization splay of a particular sign cannot fill space homogeneously but requires defects of reduced order where the opposite splay sign is found. The simplest splay organization, and the one of relevance here, has the defects as a periodic array of lines which confine splay stripes [Fig. 1(a)], with the stripe width governed by a balance of splay and defect energies. In the basic splay stripe shown in Fig. 1(a) the polarization approaches its preferred local structure in the middle of the stripe ( $x=0$ ), splaying out toward the stripe edges ( $x = \pm l/2$ ) where defects will mediate the transition to the next domain. The region of the defect comprises a structurally different environment for the molecules and thus can be expected to have, for example, different tilt from the layer normal, equilibrium layer spacing, polarization density, etc. In a bulk smectic the variation in layer spacing must be accommodated by layer undulation. For present purposes we consider two basic classes of defects, those where the smectic layering is continuous across the defect [Figs. 1(c) and 1(d)] and those where there is a half-layer step discontinuity across the defect [Figs. 1(e) and 1(f)]. The half layer step is a way to accommodate the bent-core molecular shape at the defect, tending to appear in materials with less robust layering, for example as the length of the aliphatic tails is reduced.

Taking the basic splayed layer as a tile and generating additional tiles by reflections and building the possible structures results in four general lattices illustrated in Figs. 1(g)–1(j), three of which have been observed. In this construction tilt directly determines the phase of the undulation displacement as indicated in Figs. 1(a) and 1(b), where in the  $x$ - $z$  plane the undulation phase adopted is that which tends to reduce director deformation. Within each stripe the layer normal is parallel to  $y$  at the boundary between stripes and tilts to the right (left) where the layer has negative (positive) slope. Therefore, if the molecules become less tilted at the defect, elastic energy within the middle of the stripe will be minimized if the molecules tilt to the left (right) when the layer slope is negative (positive). We label this new set of phases  $SmCPU$  where  $U$  denotes the breaking of translational symmetry within the plane of the layers by the formation of undulations. Adjacent stripes may have the same slope [ $SmCPU_S$ , Figs. 1(h) and 1(i)] or opposite slope [ $SmCPU_A$ , Figs. 1(g) and 1(j)].

The combination of polarization orientation and tilt determine the stripe chirality. Adjacent stripes may have the same chirality in which case the defect between them is  $[S]$ -type [Figs. 1(c) and 1(e)] or they may have opposite chirality in which case the defect is  $[A]$ -type [Figs. 1(d) and 1(f)]. The

TABLE I. Lattice constants for *B7* and *B1* compounds. The materials are grouped into three types:  $\text{SmCPU}_A$  phases,  $\text{SmCPU}_S$  phases, and  $\text{SmCPU}_{S'}$  phases.

Compound	$q_s$ ( $\text{\AA}^{-1}$ )	$q_m$ ( $\text{\AA}^{-1}$ )	$\gamma$ (deg)
<b>MHOBOW</b> [14]	0.1575	0.0220	90.0
<b>PBCOB</b> [16]	0.1630	0.0221	90.0
<b>H87</b> [17]	0.1374	0.0146	90.0
<b>Citro</b> [18]	0.1664	0.0227	90.0
<b>UD50</b> [19]	0.1378	0.0831	81.9
<b>M535</b> [20]	0.1599	0.0731	83.5
<b>M763</b> [20]	0.1774	0.0853	82.3
<b>2299</b> [10]	0.1330	0.0584	84.5
<b>W1044</b> [8]	0.1821	0.0694	87.3
<b>10WBVI</b> [21]	0.1239	0.0165	81.2

molecules on either side of the  $[S]$  defect tilt in opposite directions whereas the molecules on either side of the  $[A]$  defect tilt in the same direction. Clearly these two defects are structurally distinct and must therefore have different energy costs,  $U_S$  and  $U_A$ . In the case that  $U_S > U_A$ , a purely chiral phase results which we label  $\text{SmCPU}[S]$ . In the opposite limit, only  $[A]$ -type defects are present leading to a racemic structure,  $\text{SmCPU}[A]$ . Somewhat surprisingly, both defects appear in the structure of **MHOBOW**, making that structure  $\text{SmCPU}_A[SA]$ . We conclude that in materials in which the polar order is pronounced enough to enforce splay of the polarization, a number of different subphases may form depending upon the relative energies of the defects between the splay stripes. This enables us to account for most of the *B7* and *B1* structures reported.

The three most simple  $\text{SmCPU}_A$  phases ( $\text{SmCPU}_A[S]$ ,  $\text{SmCPU}_A[A]$ , and  $\text{SmCPU}_A[SA]$ , Fig. 1(g)) are primarily distinguishable via their optical properties.  $\text{SmCPU}_A[S]$  is macroscopically chiral and so a bulk sample composed of achiral molecules will be composed of equal volumes of chiral domains of opposite handedness, each with well defined optical activity. The  $\text{SmCPU}_A[A]$  phase is the only  $\text{SmCPU}_A$  phase with a macroscopic dipole and should have large second harmonic generation properties roughly comparable to that of the lamellar  $\text{SmC}_S P_F$  and  $\text{SmC}_A P_F$  phases [6–8]. The optical properties of the  $\text{SmCPU}_A[SA]$  phase have previously been predicted and verified in racemic **MHOBOW** [4].

We performed detailed x-ray scattering studies on a wide array of bent-core compounds reported to exhibit the *B7* and *B1* phases listed in Table I. These measurements were all performed on un-aligned “powder” samples contained in 0.7–1.0 mm diameter 10  $\mu\text{m}$  thick glass capillaries at the X10A beamline of the National Synchrotron Light Source. Samples were mounted in a temperature controlled Instec hotstage on a Huber 4-circle goniometer. By utilizing a Germanium analyzer, we obtained a resolution of  $\sim 3.5 \times 10^{-4} \text{\AA}^{-1}$ . All samples were heated into the isotropic phase and cooled into the *B7/B1* phase prior to measurement.

The powder patterns of all compounds were indexed to 2D lattices as tabulated in Table I. Three general structures result from this indexing: one rectangular lattice and two oblique—the oblique lattices being distinguishable by their form factors. For the materials with rectangular lattices, the indexing is straightforward with the  $s=1$ ,  $m=\pm 1$  peaks having the largest intensity (and being indistinguishable in powder scattering). When indexing the powder patterns of materials with oblique reciprocal lattices, we choose that the brightest reflection corresponds to ( $m=0$ ,  $s=1$ ). In all cases, this corresponds to the short axis of the 2D real-space lattice, as expected for materials with smecticlike order. For simplicity, we then choose that the angle  $\gamma$  between the  $q_s$  and  $q_m$  lattice vectors is less than  $90^\circ$ . The lattice indexing results in the lattice parameters,  $q_s$ ,  $q_m$ , and  $\gamma$  as well as the scattered intensity  $I(m, s)$  at each reciprocal lattice point.

The  $I(m, s)$  data of all compounds with a rectangular lattice are well fit by the form factor of a sinusoidal undulation as shown for **MHOBOW** and **PBCOB** in Figs. 2(a) and 2(b). The experimental data are normalized such that the brightest peak ( $s=1$ ,  $m=1$ ) has unit intensity. We fit these intensities to the form factor of an undulated smectic layer as described in reference [4]. We normalized the  $s=1$  and  $s=2$  peaks of the model independently so that the model intensity at  $s=1$ ,  $m=1$  and  $s=2$ ,  $m=2$  matches the experimental data. All remaining peaks are fit by adjusting a single parameter,  $A$ , which is the amplitude of the undulation. With the exception of the  $s=2$ ,  $m=0$  peak, each compound is well fit by this simple model of a sinusoidal undulation. We assume that we would obtain a better fit by including higher frequency contributions to the shape of the undulation ( $2q_m$ ,  $3q_m$ , etc.). In this analysis we neglected the effect of the powder averaging on the relative intensities of the peaks. However, because we are only comparing the intensities within each (separately normalized) group of  $m$ -indexed peaks, this amounts to at most a 10–15 % error in the relative peak intensity when viewed at the logarithmic scale.

We see from the data for **MHOBOW** and **PBCOB** that a small change in the amplitude of the undulation qualitatively changes the character of the form factor, for example  $I(m=2, s=2) > I(m=3, s=2)$  for **MHOBOW** and this is reversed for **PBCOB**. We wish to avoid the necessity of determining  $A$  in assigning the structure of the phase, so we would like a model for the form factor of a stripe that replicates the gross features of the phases, but which requires minimal knowledge about the exact form of the undulation or of the defects between stripes. To this end, we approximate the electron density of each splay stripe (half cycle in the undulation) by a rectangular block uniform in  $y$  and with a gaussian profile in  $x$  and  $z$ :

$$\rho(x, z) = \Theta(z - d/2)\Theta(z + d/2)\exp(-\omega^2 z^2) \times \Theta(x - l/2)\Theta(x + l/2)\exp(-\sigma^2 x^2), \quad (1)$$

where  $d$  is the thickness of the smectic layer,  $l$  is the width of the stripe, and  $\Theta$  is the step function. We choose  $\omega$  to be sufficiently large and  $\sigma$  to be sufficiently small to approximate well defined layering in  $z$  with fluidlike order along  $x$

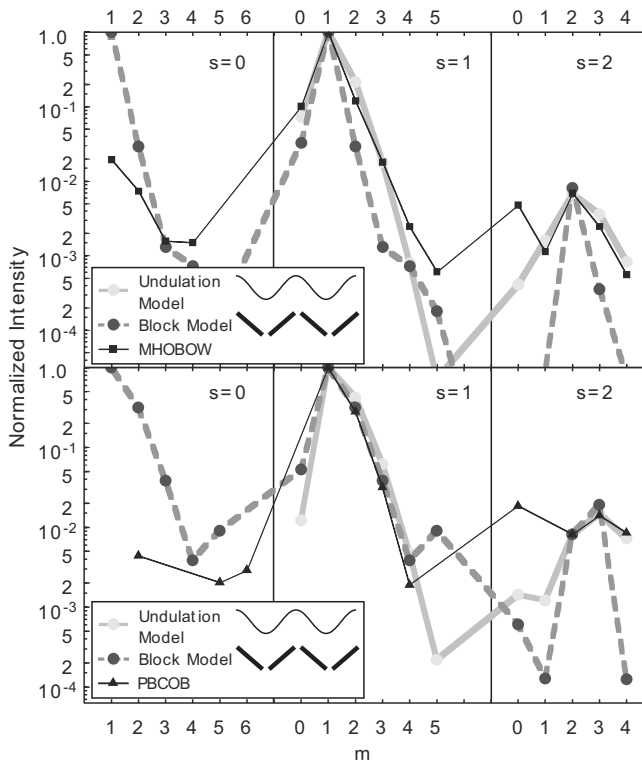


FIG. 2.  $\text{SmCPU}_A$  phases. Scattered intensity vs reciprocal lattice index  $[I(m,s)]$  for  $B7$  compounds with rectangular lattices. Data points are connected for convenience and all data have been normalized such that the  $m=1, s=1$  peak has magnitude 1. The intensity profile of the  $s=1$  peaks is qualitatively identical for all phases with the  $B7$  texture and a rectangular lattice. The thick solid line indicates an analytic calculation of the intensities from an undulated smectic layer. The thick dashed line indicates a calculation where each half cycle of the undulation (a single splay stripe) is approximated as a rectangular block. (a) **MHOBOW**. Data are best fit with  $q_s A = 1.6$ . The angular orientation of the blocks is calculated from  $\cos^{-1}(A/q_m)$  and this form factor qualitatively reproduces the analytic model. (b) **PBCOB**. Data are best fit with  $q_s A = 2.1$  and, again, the block model qualitatively reproduces the relative intensities of the peaks. The undulated smectic layer model makes no prediction about the  $s=0$  intensities and both models underestimate the intensity of the  $I(0,2)$  peak.

( $\omega=10, \sigma=0.01$ ); however, it turns out that the results do not depend strongly on these two parameters. The Fourier transform of Eq. (1) can be calculated directly and then rotated about  $\mathbf{y}$  by an angle  $\alpha$  in order to approximate the undulation as shown in the insets to Figs. 2(a) and 2(b). The quantities  $d$  and  $l$  are computed from the lattice vectors  $q_s$  and  $q_m$  respectively and  $\alpha = \tan^{-1}(Aq_m/2\pi)$ . With  $A$  taken from the fitted results from the undulated model, the resulting intensity qualitatively matches both the data and undulated model as shown in Figs. 2(a) and 2(b). In both cases the block model reproduces the qualitative form of  $I(m,s)$  with one parameter  $A$  which is fixed by the previous fit to the undulated model.

In constructing the two oblique lattices of splay stripes we point out that whereas the  $\text{SmCPU}_A$  structure contains equal numbers of stripes with positive and negative slopes [Figs. 1(f) and 1(i)], the  $\text{SmCPU}_S$  structures possess a smaller unit cell including only stripes with one sign of slope as shown in

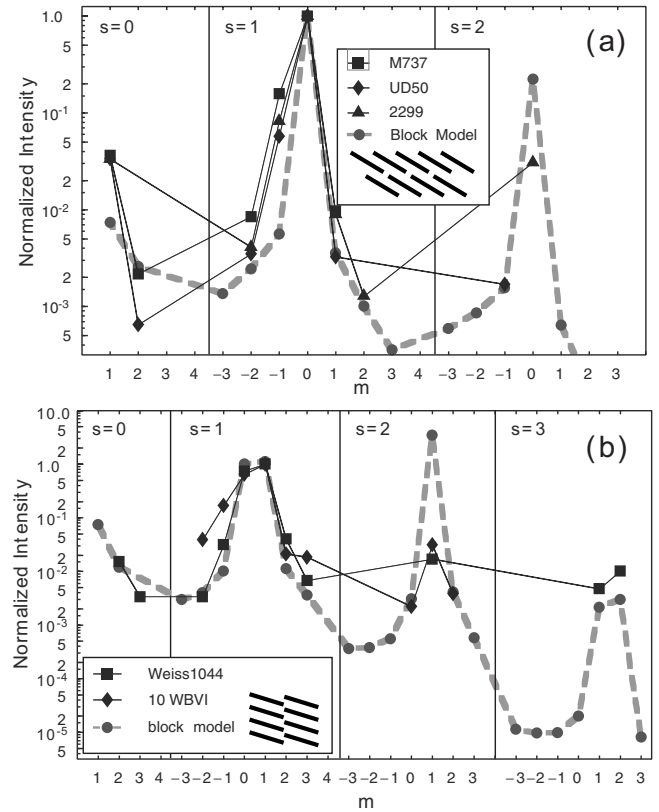


FIG. 3. (a)  $\text{SmCPU}_S$  phases  $I(m,s)$  for  $B7$  compounds with oblique reciprocal lattices and layering which is approximately continuous at the defect [Fig. 1(g)].  $\text{SmCPU}_{S'}$  phases.  $I(m,s)$  for  $B7$  compounds with oblique reciprocal lattices, and a half-layer step at the defect [Fig. 1(h)].

Figs. 1(g) and 1(h). Furthermore, in contrast to the  $\text{SmCPU}_A$  phase which has a free parameter  $A$ , we can compute the angular orientation of the blocks  $\alpha$  solely from the lattice parameters ( $\alpha = \pi/2 - \gamma$ ) which were determined in the indexing of the lattice; i.e., in this case, the amplitude of the undulation  $A$  is fixed by the lattice parameters. Figure 3(a) shows  $I(m,s)$  for the group of compounds which are well fit by the  $\text{SmCPU}_S$  structure. Interestingly, because the angular orientation of the block is determined by the lattice parameters,  $I(m,s)$  is universal for these compounds to the extent that the stripes may be assumed to undulate with exactly the same, roughly sinusoidal, shape.

Finally we turn to **W1044** [9], which exhibits classic  $B7$  textures but does not have a simple  $\text{SmCPU}_A$  undulation lattice. Rather the 2D modulation in **W1044** is similar to the  $\text{SmCPU}_S$  with a half layer step in the smectic layering at the defect boundaries as shown in Figs. 1(e), 1(f), and 1(h). We denote this phase  $\text{SmCPU}_{S'}$ , and again  $\alpha$  is determined by the lattice constants and we plot the block model form factor along with the experimental  $I(m,s)$  data for the two compounds which fit this model in Fig. 3(b). We note that this has exactly the symmetry of the  $B_{1\text{REV TILT}}$  phase structure [10] and the  $B_{1t}$  phase structure [11], i.e., polarization splay is required by symmetry for the proposed structure of these phases [12] but we assert that splay is in fact one of the basic driving mechanisms. Similarly, these structures are similar to

those proposed by Folcia *et al.* [13], but their structures require an additional broken symmetry. That is, they show identical numbers of right tilted and left tilted columns inhabiting an oblique lattice whereas in we point out that barring an additional broken symmetry, equal numbers of right and left tilted columns will yield a rectangular lattice and an oblique lattice is compatible with synclinic columns.

The  $\text{SmCPU}_S$  and  $\text{SmCPU}_{S'}$  phases are expected to have the same possibilities for defects ( $[S']$ ,  $[A']$  for the  $\text{SmCPU}_{S'}$  phase) as are found in the  $\text{SmCPU}_A$  structures as illustrated in Figs. 1(d) and 1(e). The  $\text{SmCPU}_S[S]$  and  $\text{SmCPU}_{S'}[S']$  phases are both macroscopically polar and should produce SHG light with strength comparable to that of the  $\text{SmCPU}_A[A]$  phase. They are also chiral and bulk samples of achiral molecules should thus be composed of equal volumes of optically active domains. The  $\text{SmCPU}_S[A]$  and  $\text{SmCPU}_{S'}[A']$  phases are racemic and macroscopically nonpolar. Further experiments are required to find specific instances of the remaining phases. A major caveat when describing the optical properties of these phases between crossed polarizers is the importance of knowing the orientation of the lattice. In typical smectic liquid crystals, the familiar circular focal conic provides a ready reference for the layer normal which is radial. Therefore molecular tilt is apparent as the extinction brushes are not parallel to the polarizer or analyzer. However, with these 2D lattices, it is necessary to determine the orientation of the lattice vectors with respect to the polarization direction of the light in order to determine the tilt of the molecules. Furthermore, in all three  $\text{SmCPU}$  structures, the molecules are tilted with respect to the local layer normal within the middle of the stripe. This is required by symmetry, but is not necessarily large.

An additional feature of the block model borne out by experiment is the observation that some peaks are much more intense than others, and that the intense x-ray reflections exhibit much weaker temperature dependence of peak position than the weak reflections. In the block model the block form factor is strongly peaked in the direction of the layer normal within the block, and the reflections in this direction, due to the lamellar repeat distance of the layering within the block, are correspondingly intense. Since the layer spacing is typically only weakly temperature dependent, the peak positions of these strong reflections do not change much with temperature. On the other hand, the in-plane lattice parameter and the oblique lattice angle are temperature dependent, leading to a much stronger variation of position of the weak reflections that typically depend on these parameters. This remarkable contrast is illustrated in Fig. 4.

We have found a family of phases in which the defining feature is the expression of polarity through spontaneous splay accommodated by periodic splay stripes. These polarization splay phases may have rectangular reciprocal space lattices ( $\text{SmCPU}_A$ ) in which case the phase is well described by a stack of sinusoidally undulating smectic layers. In addition, two types of oblique lattices are possible:  $\text{SmCPU}_S$  in which the smectic layers are still approximately continuous but in which the undulation only evolves through one half cycle before repeating, and  $\text{SmCPU}_{S'}$  which is identical to  $\text{SmCPU}_S$  except that at the defect boundary the molecules in

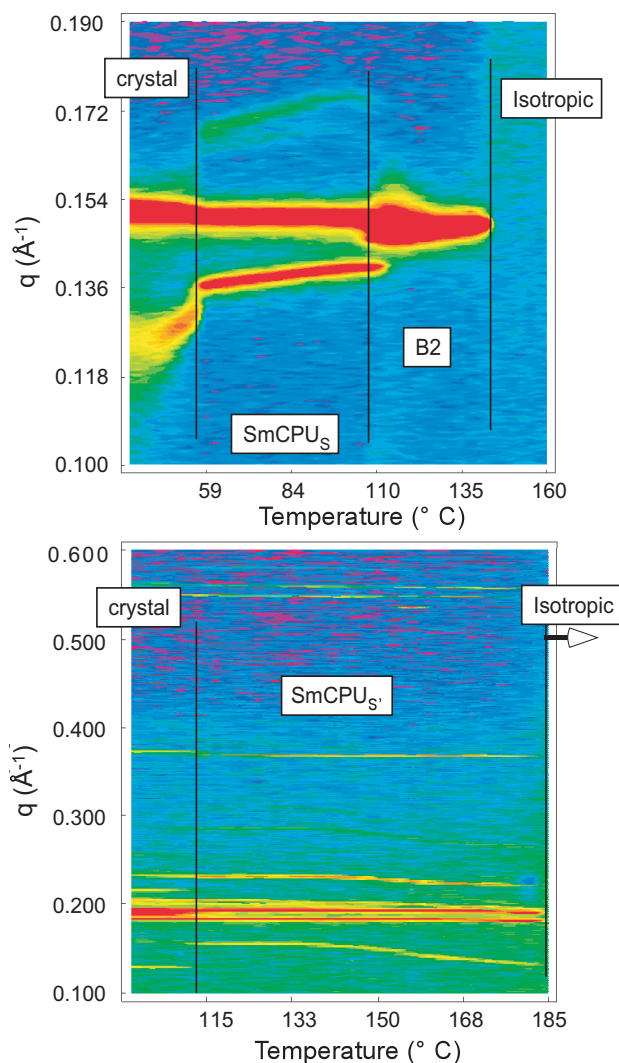


FIG. 4. (Color) Contour plots of the log of the scattered intensity (a.u.) vs temperature and wave vector. (a) **UD50**. The single strong scattering peak at  $0.15 \text{ \AA}^{-1}$  associated with the smectic layering does not change significantly in intensity or position as a function of temperature. This is characteristic of the  $\text{SmCPU}_S$  phase. (b) **W1044** the two peaks at  $0.18$  and  $0.185$  associated with the smectic layering do not change significantly with temperature. This is the hallmark of the  $\text{SmCPU}_{S'}$  phase. Note: These experiments require long term exposure of the sample to intense x-ray radiation and elevated temperatures. The expose causes the phase transition temperatures to drift over the course of the experiment but the qualitative behavior remains unchanged.

adjacent stripes interdigitate such that there is a half-layer step in the smectic layering. A diverse array of molecules expressing these phases all produce similar lattice constants but the three phases are readily distinguishable via x-ray scattering. We have limited our considerations here to phases describable by continuous and half-step layer defect structures. *B1* phases with partial layer steps have recently been found [15].

In summary, the common property of these phases is the expression of polarity through the formation of polarization splay stripes but the subphases are in fact distinct, each with distinct symmetry. We have identified four features of splay

stripes, each with two possible values: undulation direction (up versus down), polarization direction ( $\pm y$ ), layer chirality on either side of the defect (same chirality versus opposite chirality), and continuity of the smectic layering at the discontinuity (continuous versus interdigitation). The relative energy cost of these various choices determines the macroscopic structure of phase composed of splay stripes. This model describes a large number of bent-core compounds

with 2D reciprocal lattices which are reported to exhibit the *B7* and *B1* textures. In the determination of the structure of these phases, it is critical to address the form factor in addition to the lattice structure.

This work supported by NSF MRSEC Grant No. DMR-0213918 and NSF Grant No. DMR-0072989.

- 
- [1] T. Akutagawa, Y. Matsunaga, and K. Yasuhara, *Liq. Cryst.* **17**, 659 (1994).
- [2] D. Link, G. Natale, R. Shao, J. Maclennan, N. Clark, E. Korblöva, and D. Walba, *Science* **278**, 1924 (1997).
- [3] D. A. Coleman, C. D. Jones, M. Nakata, and N. A. Clark, Polarization Splay Modulated Phases Using Elastic and Defect Free Energy to Understand B1 and B7 Phases, in *Abstracts of the 10th International Conference on Ferroelectric Liquid Crystals*, Stare Jablonki, Poland (2005), p. 16.
- [4] D. A. Coleman *et al.*, *Science* **301**, 1204 (2003).
- [5] M. A. Handschy, N. A. Clark, and S. T. Lagerwall, *Phys. Rev. Lett.* **51**, 471 (1983).
- [6] M. Nakata, D. R. Link, F. Araoka, J. Thisayukta, Y. Takanishi, K. Ishikawa, J. Watanabe, and H. Takezoe, *Liq. Cryst.* **28**, 1301 (2001).
- [7] R. Macdonald, F. Kentischer, P. Warnick, and G. Heppke, *Phys. Rev. Lett.* **81**, 4408 (1998).
- [8] E. Gorecka, D. Pocięcha, F. Araoka, D. R. Link, M. Nakata, J. Thisayukta, Y. Takanishi, K. Ishikawa, J. Watanabe, and H. Takezoe, *Phys. Rev. E* **62**, R4524 (2000).
- [9] G. Pelzl, S. Diele, A. Jákli, C. Lischka, I. Wirth, and W. Weissflog, *Liq. Cryst.* **26**, 135 (1999).
- [10] J. Szydłowska, J. Mieczkowski, J. Matraszek, D. W. Bruce, E. Gorecka, D. Pocięcha, and D. Guillon, *Phys. Rev. E* **67**, 031702 (2003).
- [11] K. Pelz, W. Weissflog, U. Baumeister, and S. Diele, *Liq. Cryst.* **30**, 1151 (2003).
- [12] Any striped phase populated by polar molecules with average polar director oriented parallel to the stripes must exhibit splay. The region at the boundary between stripes presents an environment that is structurally distinct from the region in the middle of the stripe and so in general one end of the polar molecule will have a lower free energy within this region. This lowering of the free energy acts as an effective polar anchoring energy that tends to turn the polarization at the edge of the stripe either toward or away from the stripe edge, thus imposing splay.
- [13] C. L. Folcia, J. Etxebarria, J. Ortega, and M. B. Ros, *Phys. Rev. E* **72**, 041709 (2005).
- [14] D. M. Walba, E. Korblöva, R. Shao, J. E. Maclennan, D. R. Link, M. A. Glaser, and N. A. Clark, *Science* **288**, 2181 (2000).
- [15] N. Vaupotič, M. Čopič, E. Gorecka, and D. Pocięcha, *Phys. Rev. Lett.* **98**, 247802 (2007).
- [16] C. K. Lee and L. C. Chien, *Liq. Cryst.* **26**, 609 (1999).
- [17] A. Eremin, S. Diele, G. Pelzl, H. Nadasi, and W. Weissflog, *Phys. Rev. E* **67**, 021702 (2003).
- [18] M. Nakata, D. R. Link, Y. Takanishi, Y. Takahasi, J. Thisayukta, H. Niwano, D. A. Coleman, J. Watanabe, A. Iida, N. A. Clark, and H. Takezoe, *Phys. Rev. E* **71**, 011705 (2005).
- [19] G. Pelzl *et al.*, *J. Mater. Chem.* **14**, 2492 (2004).
- [20] K. Fodor-Csorba, A. Vajda, A. Jákli, C. Slugovc, G. Trimmel, D. Demus, E. Gács-Baitz, S. Holly, and G. Galli, *J. Mater. Chem.* **14**, 2499 (2004).
- [21] V. Novotna, M. Glogarova, V. Hamplova, M. Kaspar, N. A. Clark, C. D. Jones, and D. A. Coleman, The B2–B7 Transition in Bent-Shaped Mesogens with Methoxy Substitution, in *Abstracts of the 20th International Liquid Crystal Conference*, Ljubljana, Slovenia (2004), p. 983.